

Communication

Self-Standing Soft Carbon-Coated MoS₂ Nanofiber Film Anode for Superior Potassium Storage

Qinglin Deng^{1,2,*}  and Lingmin Yao^{1,2,*}

¹ School of Physics and Materials Science, Guangzhou University, Guangzhou 510006, China

² Research Center for Advanced Information Materials (CAIM), Huangpu Research & Graduate School of Guangzhou University, Guangzhou 510555, China

* Correspondence: qldeng@gzhu.edu.cn (Q.D.); lingminyao@gzhu.edu.cn (L.Y.)

Abstract: The poor electronic conductivity and large volume expansion effect of MoS₂ limit its application in potassium-ion batteries (PIBs). In addition to exploring effective modification methods, it is also necessary to build a new self-standing electrode system to improve its energy density. In this work, based on the potassium storage advantages and disadvantages of MoS₂ and carbon nanofibers, we have successfully prepared a self-standing soft carbon-coated MoS₂ nanofiber film electrode without any additives or metal collectors. As for the application in PIBs, it exhibits excellent rate performances (about 93 mA h g⁻¹ at the current density of 10 A g⁻¹), and superior long-term cycling stability performances (a high-capacity retention of ~75% after 1800 cycles at the current density of 1 A g⁻¹). The enhanced potassium storage performance can be attributed to the unique self-standing nanofiber film architectures.

Keywords: MoS₂; anode; potassium ion batteries; carbon nanofibers; self-standing



Citation: Deng, Q.; Yao, L. Self-Standing Soft Carbon-Coated MoS₂ Nanofiber Film Anode for Superior Potassium Storage. *Coatings* **2022**, *12*, 1969. <https://doi.org/10.3390/coatings12121969>

Academic Editor: Je Moon Yun

Received: 23 November 2022

Accepted: 12 December 2022

Published: 15 December 2022

Publisher's Note: MDPI stays neutral with regard to jurisdictional claims in published maps and institutional affiliations.



Copyright: © 2022 by the authors. Licensee MDPI, Basel, Switzerland. This article is an open access article distributed under the terms and conditions of the Creative Commons Attribution (CC BY) license (<https://creativecommons.org/licenses/by/4.0/>).

1. Introduction

With the widespread use of electronic products, and the growing popularity of new energy vehicles, the demand for lithium-ion batteries (LIBs) has been unprecedented. However, the global lithium resources are scarce and unevenly distributed. Moreover, the current immature battery recycling mechanism inevitably affects its cost and supply and demand [1]. To solve this problem, developing batteries with abundant resources and at a low cost is both urgent and effective. Among them, the potassium-ion batteries (PIBs), which have a similar energy storage mechanism to the LIBs, have received special attention [2–4]. Potassium is much more abundant on the earth than lithium. As compared with sodium-ion batteries (SIBs), PIBs have some unique energy storage advantages. The standard electrode potential of potassium is -2.93 V (vs. SHE), which is close to lithium (-3.04 V vs. SHE) and higher than sodium (-2.71 V vs. SHE), meaning PIBs have a higher potential energy density than SIBs [5]. In addition, potassium can form stable intercalation compounds with graphite, while sodium is difficult to insert into graphite. [6,7]

As far as the anode electrode of PIBs is concerned, its research is still in the initial stage [8]. The excellent potassium storage anodes have characteristics similar to those of LIBs and SIBs. However, as the size of a K-ion (0.138 nm) is larger than that of a Na-ion (0.102 nm) and a Li-ion (0.076 nm), the larger potassium ion radius will result in slow ion diffusion kinetics [7,9]. According to the different potassium storage mechanisms, the anodes can be classified into three categories: alloy-type, conversion-type, and intercalation-type [10–13]. Among them, the conversion-type MoS₂ shows great structural advantages in potassium storage applications [14–16]. MoS₂ combines 2D monolayers formed by bonded Mo and S atoms, with a weak van der Waals force. Anisotropic structure provides MoS₂ with a large number of reaction sites and 2D channels to boost ion insertion/extraction and rapid electron transfer [17]. However, its poor electronic conductivity and large volume expansion effect still limit its application in PIBs. Exploring excellent modification

strategies is still a hot topic [18–20]. Additionally, in order to prepare an anode with excellent potassium storage performances, in addition to selecting a high-performance anode system, it is also necessary to build a new electrode system that is self-standing and free of adhesives, conductive additives, and metal collectors [21]. For the anode electrode, if taking the weight of the binder, the conductive agent, and the metal collector into account, its actual specific capacity will be very low [22], which will seriously restrict the energy density of the whole battery. In view of the significant advantages of MoS₂ in potassium storage, it is a challenging research topic to explore the construction method of high-performance self-standing electrodes.

In this work, we are committed to designing a self-standing MoS₂-based anode without any additives or metal collectors for the applications in PIBs. This work will explore self-standing framework and effective carbon modification strategies by combining electrospinning and hydrothermal methods.

2. Materials and Methods

Synthesis of CNFs: Firstly, we can prepare the electrospinning solution by mixing the 0.6 g of PAN (polyacrylonitrile) and 8 mL of DMF (N, N-Dimethylformamide). Then, the precursor carbon nanofibers (CNFs) can be obtained using the electrospinning method. The final CNFs are obtained by heating it in air at 250 °C for 3 h, then at 700 °C for 5 h under an argon atmosphere.

Synthesis of MoS₂@CNFs and pure MoS₂ NS: Typically, an aqueous solution (30 mL) for the reaction was prepared by mixing 0.08 g of ammonium molybdate tetrahydrate, 0.09 g of thiourea, and 0.15 g of PVP (polyvinyl pyrrolidone). Then, the appropriate amount of the as-prepared CNFs film was added into the above aqueous solution. The hydrothermal reaction conditions were set at 200 °C for 24 h. Then, the generated sample was washed and dried, and finally annealed at 700 °C for 5 h under an argon atmosphere. The pure MoS₂ nanospheres (NS) can be prepared in the absence of CNFs.

Synthesis of MoS₂@CNFs@C: Typically, the appropriate amount of the as-prepared MoS₂@CNFs film was immersed in the glucose (20 mg) aqueous solution (30 mL), and then hydrothermally reacted at 180 °C for 12 h. Then, the generated sample was washed and dried. The final MoS₂@CNFs@C can be obtained by heating it at 700 °C for 5 h under an argon atmosphere. Note that polyacrylonitrile and the other reagents were purchased from commercial sources of Aldrich and Aladdin, respectively, which are directly used without any further purification.

Characterization methods: The phase structure of samples was checked using X-ray diffraction (XRD, Rigaku, Japan). The surface morphologies of the as-prepared samples were studied using a scanning electron microscopy (SEM, SU8010, Hitachi, Japan).

Electrochemical tests: Except for the pure MoS₂ NS, the other samples were directly utilized as the working electrode in the absence of additives and metal current collectors. The pure MoS₂ NS electrode was prepared through a traditional coating process. A mixed slurry (8:1:1 by weight) of active material, carbon black, and polyvinylidene fluoride was coated on a Cu foil, and then dried at 100 °C under vacuum condition. The potassium metal disk was utilized as to counter and reference electrodes. The glass fiber membrane and the 0.8 M KPF₆ solution in a 1:1 (by volume) mixture of EC and DEC were used as the separator and the electrolytes, respectively. A two-electrode coin cell was fabricated in a glove box under an argon atmosphere with 0.1 ppm moisture and oxygen content. The galvanostatic charge-discharge (GCD) data were investigated by battery testing instruments in the current density range of 0.1–10 A g⁻¹.

3. Results and Discussion

Figure 1 schematically shows the typical preparation procedures of the MoS₂@CNFs@C sample. Firstly, the CNFs can be obtained by optimizing the electrospinning conditions. As we know, owing to the wide layer spacing and large degree of disorder, hard carbon is conducive to the intercalation of potassium ions [23–25]. The carbon nanofibers derived from

electrospinning can be used as the framework for preparing self-standing electrode. By using the hydrothermal technique and PVP, MoS₂ nanospheres (NS) can uniformly anchor to the surface of CNFs. Finally, with the aid of hydrothermal and annealing treatments, the surface of MoS₂@CNFs will be coated with soft carbon layers derived from the glucose. Such a structural design will not only effectively improve the electronic conductivity of the material but will also obtain a potassium storage electrode without any additives or metal collectors, which can be used directly to assemble a two-electrode coin-cell.

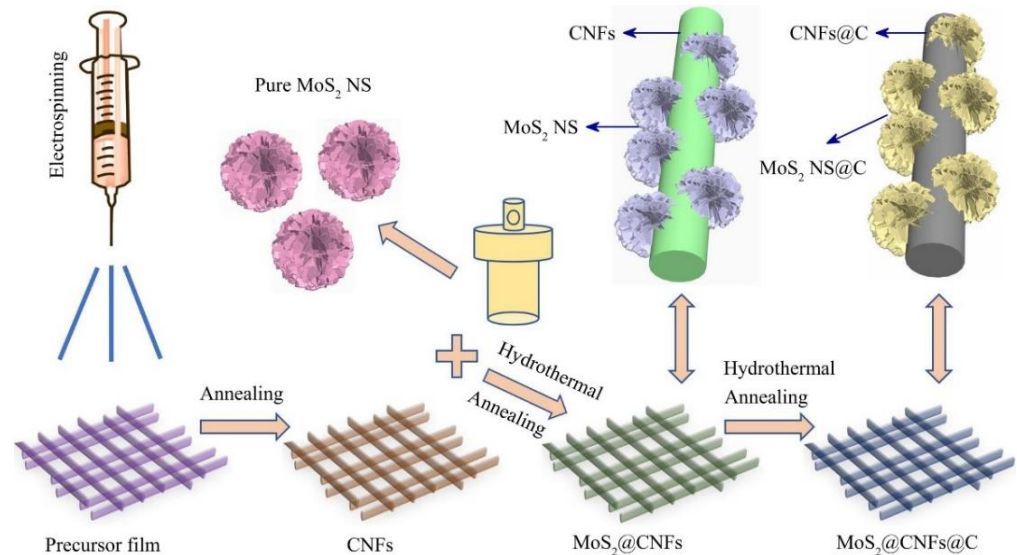


Figure 1. Schematic illustration of the fabrication of MoS₂@CNFs@C film electrode.

As shown in Figure 2, the phase structures of the samples are checked by XRD. It can be seen that the pure MoS₂ NS sample shows the characteristic (100) and (110) diffraction peaks. The MoS₂@CNFs exhibits the characteristic XRD peaks of MoS₂ without any impure phase, indicating the successful combination of MoS₂ and CNFs. After carbon coating, as compared with MoS₂@CNFs, no obvious differences in the XRD patterns are observed for MoS₂@CNFs@C, suggesting the effective carbon modification strategy.

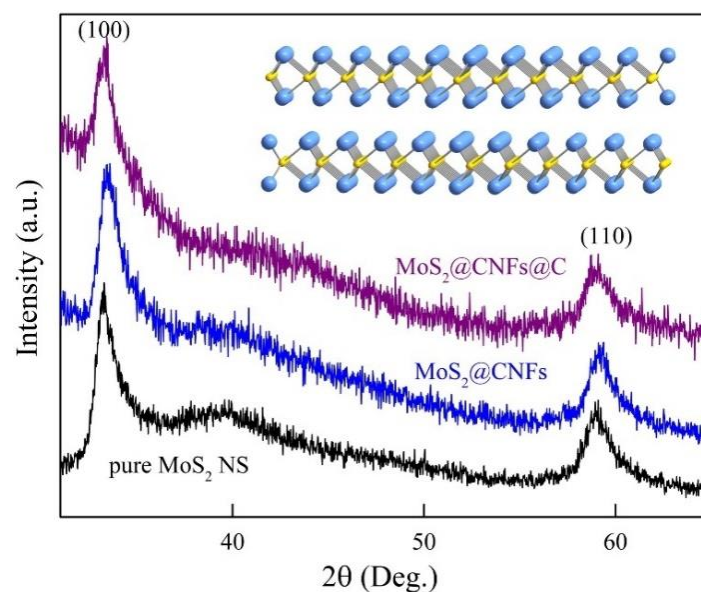


Figure 2. The XRD patterns of pure MoS₂ NS, MoS₂@CNFs, and MoS₂@CNFs@C. The inset is the simulated crystal structures of MoS₂.

Figure 3 shows the SEM images of samples. For CNFs, it can be seen that a network structure is formed by lots of nanofibers (shown in Figure 3a). After hydrothermal and annealing treatment, the MoS₂ NS are uniformly loaded onto the surface of CNFs (shown in Figure 3b). After carbon modification, MoS₂@CNFs@C can maintain the morphology structure similar to MoS₂@CNFs (shown in Figure 3c). In addition, Figure 3d shows the typical nanosheet stacking structure of a pure MoS₂ NS, which presents a nanosphere morphology. Such an assembly structure can be expected to exhibit enhanced potassium storage performances.

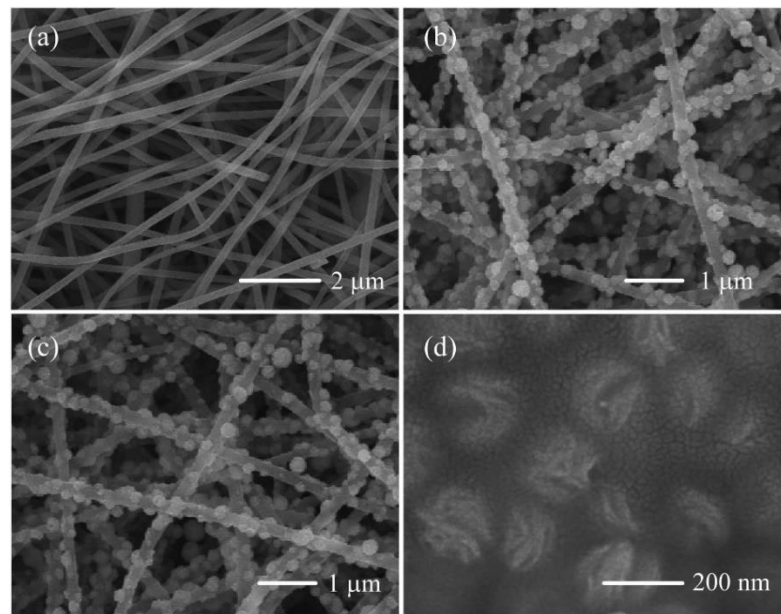


Figure 3. SEM images of (a) CNFs, (b) MoS₂@CNFs, (c) MoS₂@CNFs@C, and (d) pure MoS₂ NS.

As shown in Figure 4, this work studied the potassium storage performances of a pure MoS₂ NS electrode. It can be seen that both the rate and cycling stability performances are poor. As shown in Figure 4a, with increasing the discharge current density, the specific capacity of the electrode gradually decreases. When the current density increases to 5 A g⁻¹, the specific capacity is close to 0. It can basically return to the previous state as the current density returns to 0.2 A g⁻¹. In addition, as shown in Figure 4b, during the first 100 cycles, the specific capacity decreases rapidly. The reason for the poor rate and cycle stability performances of a pure MoS₂ NS electrode can be attributed to the poor electronic conductivity and the inevitable agglomeration phenomenon [26].

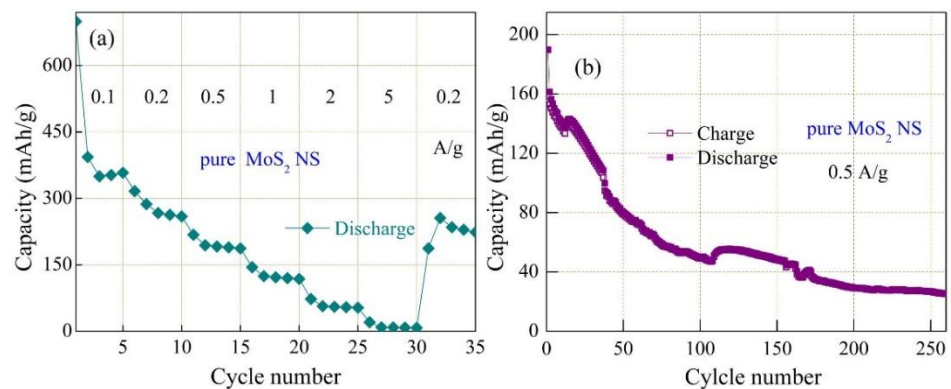


Figure 4. (a) The rate performance data of pure MoS₂ NS in range of 0.1–5 A g⁻¹. (b) The cycling stability data of pure MoS₂ NS at 0.5 A g⁻¹.

Aiming at this problem, this work proposes structural and carbon modification strategies. Figure 5a shows the rate performance of the $\text{MoS}_2@\text{CNFs}$ and $\text{MoS}_2@\text{CNFs}@C$ electrodes in the range of $0.5\text{--}10\text{ A g}^{-1}$. As we can see, the $\text{MoS}_2@\text{CNFs}@C$ electrode displays a better rate performance compared with the $\text{MoS}_2@\text{CNFs}$ electrode. Owing to the existence of the carbon layer, when the discharge current density increases to more than 5 A g^{-1} , the rate advantage of the $\text{MoS}_2@\text{CNFs}@C$ electrode begins to appear. Its specific capacity is obviously higher than that of the $\text{MoS}_2@\text{CNFs}$ electrode under the same current density. Specifically, the $\text{MoS}_2@\text{CNFs}@C$ electrode shows a specific capacity of about 208, 185, 156, 131, and 93 mA h g^{-1} at $0.5, 1, 2, 5,$ and 10 A g^{-1} , respectively. In addition, the advantages of free-standing and the carbon layer structure result in an increasingly excellent cycling stability performance. As shown in Figure 5c, when increasing the number of cycles, their specific capacities show a downward trend. It is obvious that the $\text{MoS}_2@\text{CNFs}$ electrode without carbon modification decreases quickly. After 1000 cycles, the capacity retention of the $\text{MoS}_2@\text{CNFs}$ and the $\text{MoS}_2@\text{CNFs}@C$ electrode is $\sim 54\%$ and $\sim 79\%$, respectively. The $\text{MoS}_2@\text{CNFs}@C$ electrode shows significantly better cycling stability with the slowly decreasing GCD curves (shown in Figure 5d). Even after 1800 cycles, it still has a high-capacity retention of about 75% .

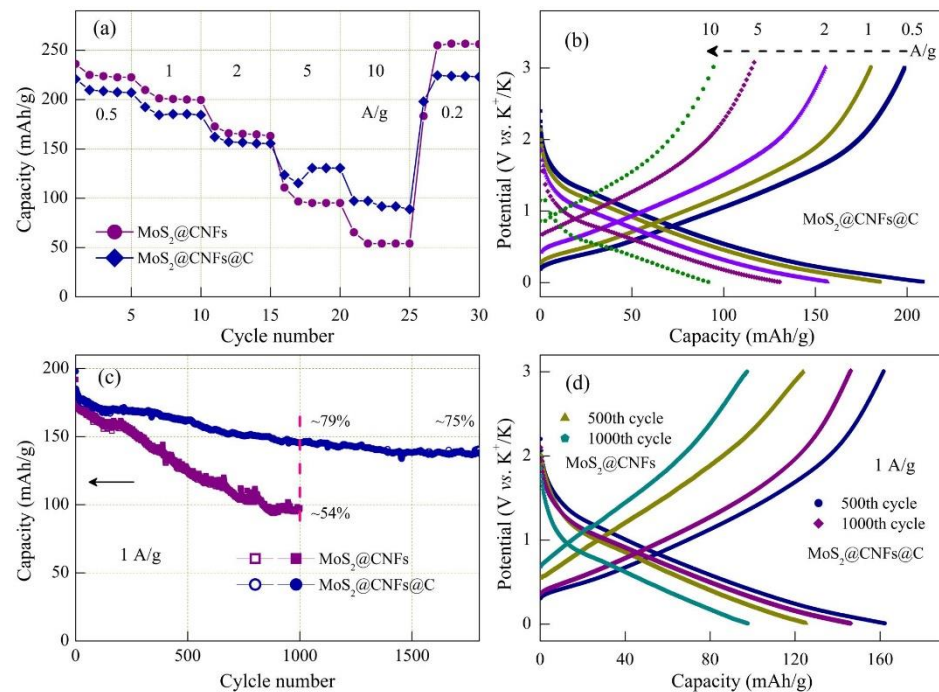


Figure 5. (a) Rate performance of $\text{MoS}_2@\text{CNFs}$ and $\text{MoS}_2@\text{CNFs}@C$ at different current densities, (b) with the corresponding GCD curves of $\text{MoS}_2@\text{CNFs}@C$. (c) Cycling stability performance of $\text{MoS}_2@\text{CNFs}$ and $\text{MoS}_2@\text{CNFs}@C$ at 1 A g^{-1} , (d) with the corresponding GCD curves of $\text{MoS}_2@\text{CNFs}$ and $\text{MoS}_2@\text{CNFs}@C$ at the 500th and 1000th cycle.

The enhanced potassium storage performances can be attributed to the unique self-standing carbon-coated $\text{MoS}_2@\text{CNFs}$ film architectures. Such a structure can effectively prevent the agglomeration behavior of the MoS_2 NS loaded on the CNFs, relax the volume expansion, and increase the contact area between active material and an electrolyte. The coated carbon layers can improve the electronic conductivity of the whole electrode. It can also inhibit structural damage of electrode materials during the charging–discharging process in PIBs. As a result, the self-standing $\text{MoS}_2@\text{CNFs}@C$ film electrode exhibits the excellent potassium storage performances.

4. Conclusions

In summary, based on the potassium storage structure advantages of MoS₂, we ingeniously designed and synthesized a novel self-standing electrode system of MoS₂@CNFs@C, without any additives or metal collectors. The carbon nanofibers derived from electrospinning were used as the self-standing skeleton for the uniform loading place of MoS₂ NS. The soft carbon layer derived from glucose can effectively improve the electronic conductivity of the whole electrode, and acts as a protective layer for electrodes. Such a structure exhibits an excellent rate performance (about 208, 185, 156, 131, and 93 mA h g⁻¹ at the current density of 0.5, 1, 2, 5, and 10 A g⁻¹, respectively,) and cycle stability performance (a high-capacity retention of ~75% after 1800 cycles at the current density of 1 A g⁻¹) as for the application in PIBs. It is believed that other types of energy-storage electrodes can benefit from the similar structure and modification strategies.

Author Contributions: Writing—original draft preparation, Q.D.; writing—review and editing, Q.D. and L.Y.; funding acquisition, Q.D. and L.Y. All authors have read and agreed to the published version of the manuscript.

Funding: This research was funded by the National Natural Science Foundation of China (No. 22109032, 51802047), Guangzhou Science and Technology Plan Project (No. 202201010327), and the Talent Cultivation Project of Guangzhou University (No. RP2021038).

Institutional Review Board Statement: Not applicable.

Informed Consent Statement: Not applicable.

Data Availability Statement: Not applicable.

Conflicts of Interest: The authors declare no conflict of interest.

References

1. Huang, B.; Pan, Z.; Su, X.; An, L. Recycling of lithium-ion batteries: Recent advances and perspectives. *J. Power Sources* **2018**, *399*, 274–286. [[CrossRef](#)]
2. Min, X.; Xiao, J.; Fang, M.; Wang, W.; Zhao, Y.; Liu, Y.; Abdelkader, A.M.; Xi, K.; Kumar, R.V.; Huang, Z. Potassium-ion batteries: Outlook on present and future technologies. *Energ. Environ. Sci.* **2021**, *14*, 2186–2243. [[CrossRef](#)]
3. Zhang, W.; Liu, Y.; Guo, Z. Approaching high-performance potassium-ion batteries via advanced design strategies and engineering. *Sci. Adv.* **2019**, *5*, eaav7412. [[CrossRef](#)] [[PubMed](#)]
4. Rajagopalan, R.; Tang, Y.; Ji, X.; Jia, C.; Wang, H. Advancements and Challenges in Potassium Ion Batteries: A Comprehensive Review. *Adv. Funct. Mater.* **2020**, *30*, 1909486. [[CrossRef](#)]
5. Pramudita, J.C.; Sehwat, D.; Goonetilleke, D.; Sharma, N. An Initial Review of the Status of Electrode Materials for Potassium-Ion Batteries. *Adv. Energy Mater.* **2017**, *7*, 1602911. [[CrossRef](#)]
6. Fan, L.; Ma, R.; Zhang, Q.; Jia, X.; Lu, B. Graphite Anode for a Potassium-Ion Battery with Unprecedented Performance. *Angew. Chem. Int. Edit.* **2019**, *58*, 10500–10505. [[CrossRef](#)] [[PubMed](#)]
7. Wu, X.; Chen, Y.; Xing, Z.; Lam, C.W.K.; Pang, S.-S.; Zhang, W.; Ju, Z. Advanced Carbon-Based Anodes for Potassium-Ion Batteries. *Adv. Energy Mater.* **2019**, *9*, 1900343. [[CrossRef](#)]
8. Xu, Y.-S.; Duan, S.-Y.; Sun, Y.-G.; Bin, D.-S.; Tao, X.-S.; Zhang, D.; Liu, Y.; Cao, A.-M.; Wan, L.-J. Recent developments in electrode materials for potassium-ion batteries. *J. Mater. Chem. A* **2019**, *7*, 4334–4352. [[CrossRef](#)]
9. Zhang, C.; Zhao, H.; Lei, Y. Recent Research Progress of Anode Materials for Potassium-ion Batteries. *Energy Environ. Mater.* **2020**, *3*, 105–120. [[CrossRef](#)]
10. Song, K.; Liu, C.; Mi, L.; Chou, S.; Chen, W.; Shen, C. Recent Progress on the Alloy-Based Anode for Sodium-Ion Batteries and Potassium-Ion Batteries. *Small* **2021**, *17*, 1903194. [[CrossRef](#)]
11. Liang, S.; Shi, H.; Yu, Z.; Liu, Q.; Cai, K.; Wang, J.; Xu, Z. Uncovering the design principle of conversion-based anode for potassium ion batteries via dimension engineering. *Energy Storage Mater.* **2021**, *34*, 536–544. [[CrossRef](#)]
12. Cao, K.; Zheng, R.; Wang, S.; Shu, J.; Liu, X.; Liu, H.; Huang, K.-J.; Jing, Q.-S.; Jiao, L. Boosting Coulombic Efficiency of Conversion-Reaction Anodes for Potassium-Ion Batteries via Confinement Effect. *Adv. Funct. Mater.* **2020**, *30*, 2007712. [[CrossRef](#)]
13. Li, N.; Zhang, F.; Tang, Y. Hierarchical T-Nb₂O₅ nanostructure with hybrid mechanisms of intercalation and pseudocapacitance for potassium storage and high-performance potassium dual-ion batteries. *J. Mater. Chem. A* **2018**, *6*, 17889–17895. [[CrossRef](#)]
14. Zheng, N.; Jiang, G.; Chen, X.; Mao, J.; Zhou, Y.; Li, Y. Rational design of a tubular, interlayer expanded MoS₂-N/O doped carbon composite for excellent potassium-ion storage. *J. Mater. Chem. A* **2019**, *7*, 9305–9315. [[CrossRef](#)]
15. Xie, K.; Yuan, K.; Li, X.; Lu, W.; Shen, C.; Liang, C.; Vajtai, R.; Ajayan, P.; Wei, B. Superior Potassium Ion Storage via Vertical MoS₂ “Nano-Rose” with Expanded Interlayers on Graphene. *Small* **2017**, *13*, 1701471. [[CrossRef](#)]

16. Li, J.; Rui, B.; Wei, W.; Nie, P.; Chang, L.; Le, Z.; Liu, M.; Wang, H.; Wang, L.; Zhang, X. Nanosheets assembled layered MoS₂/MXene as high performance anode materials for potassium ion batteries. *J. Power Sources* **2020**, *449*, 227481. [[CrossRef](#)]
17. Chong, S.; Sun, L.; Shu, C.; Guo, S.; Liu, Y.; Wang, W.; Liu, H.K. Chemical bonding boosts nano-rose-like MoS₂ anchored on reduced graphene oxide for superior potassium-ion storage. *Nano Energy* **2019**, *63*, 103868. [[CrossRef](#)]
18. Jia, B.; Yu, Q.; Zhao, Y.; Qin, M.; Wang, W.; Liu, Z.; Lao, C.-Y.; Liu, Y.; Wu, H.; Zhang, Z.; et al. Bamboo-Like Hollow Tubes with MoS₂/N-Doped-C Interfaces Boost Potassium-Ion Storage. *Adv. Funct. Mater.* **2018**, *28*, 1803409. [[CrossRef](#)]
19. Hu, J.; Xie, Y.; Zhou, X.; Zhang, Z. Engineering Hollow Porous Carbon-Sphere-Confined MoS₂ with Expanded (002) Planes for Boosting Potassium-Ion Storage. *ACS Appl. Mater. Interfaces* **2020**, *12*, 1232–1240. [[CrossRef](#)]
20. Cui, Y.; Liu, W.; Feng, W.; Zhang, Y.; Du, Y.; Liu, S.; Wang, H.; Chen, M.; Zhou, J. Controlled Design of Well-Dispersed Ultrathin MoS₂ Nanosheets inside Hollow Carbon Skeleton: Toward Fast Potassium Storage by Constructing Spacious “Houses” for K Ions. *Adv. Funct. Mater.* **2020**, *30*, 1908755. [[CrossRef](#)]
21. Deng, Q.; Fu, Y.; Zhu, C.; Yu, Y. Niobium-Based Oxides Toward Advanced Electrochemical Energy Storage: Recent Advances and Challenges. *Small* **2019**, *15*, 1804884. [[CrossRef](#)] [[PubMed](#)]
22. Xu, Y.; Zhu, Y.; Han, F.; Luo, C.; Wang, C. 3D Si/C Fiber Paper Electrodes Fabricated Using a Combined Electro-spray/Electrospinning Technique for Li-Ion Batteries. *Adv. Energy Mater.* **2015**, *5*, 1400753. [[CrossRef](#)]
23. Chen, C.; Wang, Z.; Zhang, B.; Miao, L.; Cai, J.; Peng, L.; Huang, Y.; Jiang, J.; Huang, Y.; Zhang, L.; et al. Nitrogen-rich hard carbon as a highly durable anode for high-power potassium-ion batteries. *Energy Storage Mater.* **2017**, *8*, 161–168. [[CrossRef](#)]
24. Chen, M.; Wang, W.; Liang, X.; Gong, S.; Liu, J.; Wang, Q.; Guo, S.; Yang, H. Sulfur/Oxygen Codoped Porous Hard Carbon Microspheres for High-Performance Potassium-Ion Batteries. *Adv. Energy Mater.* **2018**, *8*, 1800171. [[CrossRef](#)]
25. Cui, R.C.; Xu, B.; Dong, H.J.; Yang, C.C.; Jiang, Q. N/O Dual-Doped Environment-Friendly Hard Carbon as Advanced Anode for Potassium-Ion Batteries. *Adv. Sci.* **2020**, *7*, 1902547. [[CrossRef](#)]
26. Wang, T.; Chen, S.; Pang, H.; Xue, H.; Yu, Y. MoS₂-Based Nanocomposites for Electrochemical Energy Storage. *Adv. Sci.* **2017**, *4*, 1600289. [[CrossRef](#)]